American Mineralogist, Volume 67, pages 284–291, 1982

Orientation and effects of channel H_2O and CO_2 in cordierite

THOMAS ARMBRUSTER[1] AND F. D. BLOSS

Department of Geological Sciences
Virginia Polytechnic Institute and State University
Blacksburg, Virginia 24061

Abstract

Channel CO_2 and H_2O has been re-introduced into a channel evacuated Mg-cordierite

$$K_{0.01}Na_{0.03}(Mg_{1.91}Fe_{0.09}Mn_{0.01})Al_{3.98}Si_{5.01}O_{18}$$

from White Well, Australia. At 600°C and pressures up to 6 kbar, a maximum of 3.13 wt.% CO_2 and 2.6 wt.% H_2O re-enter cordierite's channels. The H_2O molecule orients preferentially with its H–H vector parallel to c (optic orientation: $c = X$, $b = Y$, $a = Z$). With increased H_2O content, the refractive indices γ and β increase more strongly than α whereas the a_0 cell edge decreases, b_0 perhaps increases slightly, and c_0 first increases and then levels off. The linear CO_2 molecule orients chiefly parallel to cordierite's a-axis so that, as CO_2 content increased, refractive index γ increased more strongly than did α and β. As a result, $2V_x$ increased with CO_2 content so as to exceed 90°. Simultaneously, c_0 increased, a_0 decreased, and b_0 remained constant. The distortion index Δ for these crystals changed with H_2O and CO_2 content.

Introduction

Cordierites, $Na_{x+2y}(Mg,Fe,Mn)^{VI}_{2-y}(Al_{4-x}Be_x Si_5)^{IV}O_{18} \cdot n[H_2O,CO_2]$, consist structurally of six-membered rings of corner-sharing tetrahedra (T_2 in Fig. 1) stacked along the c-axis. These are linked (laterally and vertically) by corner-sharing with other tetrahedra (T_1) to form a framework structure (Gibbs, 1966). The ring-stacking produces channels along the c-axis that pinch to 'bottlenecks' (~2.5Å in diameter) or swell to large 'cages' whose maximum dimensions, which occur in the plane parallel to (001), are approximately 5.4Å along b and 6.0Å along a. In low cordierite, Al concentrates into the two equivalent T_26 tetrahedra in the $Al_2Si_4O_{18}$ ring so that, instead of possessing a 6-fold axis, as for the Si_6O_{18} ring in beryl, the $Al_2Si_4O_{18}$ ring possesses a 2-fold axis (like that drawn perpendicular to the lightly stippled plane in Fig. 1). This leads to the orthorhombic symmetry ($Cccm$, $Z = 4$, $a > b > c$) thus far exhibited by cordierites from metamorphic and igneous rocks (Selkregg and Bloss, 1980; Wallace and Wenk, 1980). High-cordierite or indialite, found where shale and sandstone fused near a burning coal seam (Miyashiro and Iiyama, 1954), appears to be hexagonal, the rapid cooling apparently preventing Al from concentrating in T_26. Such also seems the case for cordierites from meteorites or those synthesized by recrystallization from a glass (Schreyer and Schairer, 1961), by growth in a flux (Lee and Pentecost, 1976), and by hydrothermal methods (Schreyer and Yoder, 1964). Additional heating of such synthetics leads to Si/Al ordering accompanied by twinning along (110) and (310) (Putnis, 1980; Armbruster and Bloss, 1981).

In natural cordierites the structural channels accommodate numerous species of which CO_2 and H_2O can be recognized by IR spectroscopy, and He and Ar by mass spectrometry (Damon and Kulp, 1958; Beltrame *et al.*, 1976). Hydrocarbons and other gases may also be present in small concentrations not revealed in IR spectra. Na^+ is an important channel occupant that centers in the bottlenecks (Meagher, 1967) and provides charge balance if Be^{2+} substitutes for Al^{3+} (Povondra and Langer, 1971). Small amounts of Fe in the channels may cause the pleochroism of some cordierites (Goldman *et al.*, 1977), but firm data in support of this are not yet at hand.

The degree of variation of the cordierite lattice from hexagonal symmetry is customarily measured

---

[1] Present address: Laboratory for Chemical and Mineralogical Crystallography, University of Bern, Freiestrasse 3, CH-3012 Bern, Switzerland.

0003–004X/82/0304–0284$02.00

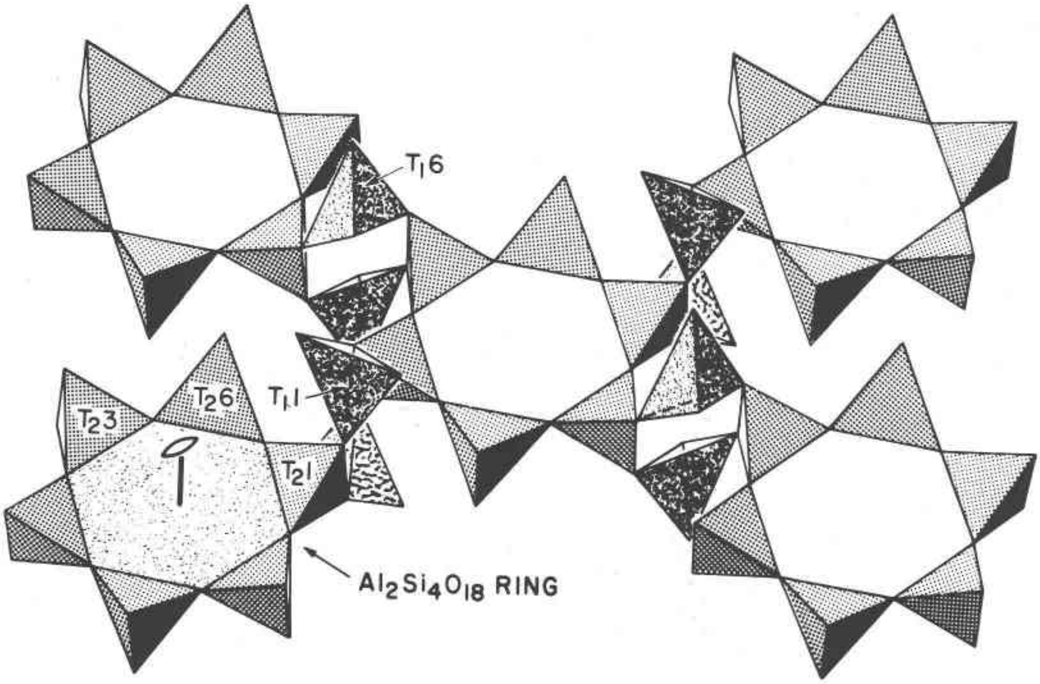

Fig. 1. Part of the cordierite framework (after Gibbs, 1966). The rings consisting of six (unstippled) tetrahedra are linked to each other, both laterally and vertically, by sharing corners with the darkly stippled tetrahedra. At the lower left, the *c*-axis (9.3Å repeat) is shown centered in one of the $Al_2Si_4O_{18}$ rings. For orthorhombic cordierites, tetrahedral sites T_21, T_26 and T_23 (symbolism of Meagher and Gibbs, 1977) are non-equivalent because Al concentrates in T_26. Also, T_11 and T_16 are non-equivalent because Al concentrates in T_11. In consequence the *c*-axis is 2-fold.

by the distortion index Δ, which Miyashiro (1957) defined (for Cu$K\alpha$ radiation) as

$$\Delta = 2\theta_{131} - (2\theta_{511} + 2\theta_{421})/2.$$

The assumption was then made that Δ provided a reliable measure of Al/Si ordering for natural cordierites. However, systematic optical and X-ray studies of natural and heated cordierites (Selkregg and Bloss, 1980) has shown this to be unlikely for natural cordierites, excluding indialites. Instead, the Δ index depended on Na-content, Fe- and Mn-substitution for Mg, and on water content. Although degrees of Si/Al ordering would without doubt influence Δ, cordierites from metamorphic and igneous rocks appear to have cooled so slowly that, thus far, all crystal structure analyses (Gibbs, 1966; Cohen, *et al.*, 1977; Hochella *et al.*, 1979; Wallace and Wenk, 1980) have disclosed nearly perfect Si/Al ordering.

In studies of natural cordierites, the tendency has been to overlook all channel occupants except H_2O. However, CO_2 also seems important (Suknev *et al.*, 1971; Schreyer *et al.*, 1979; Hörmann *et al.*, 1980) and leads to specific distortions of the cordierite lattice and modifications of its optical properties (Armbruster and Bloss, 1980). The present paper examines the effects of the orientation of H_2O and CO_2 on the crystal lattice and optical properties of a cordierite with a well ordered Si/Al distribution.

Experimental

A Mg-cordierite from White Well, Australia (Pryce, 1973) with well ordered Si/Al distribution (Cohen *et al.*, 1977; Hochella *et al.*, 1979) was crushed to an average grain size of about 200 μm. Transparent, inclusion-free grains were hand picked under a binocular microscope and tempered for one day between 1200°C and 1300°C in a SiC-furnace in order to expel the volatile channel occupants. Electron microprobe and coulombmetrical analyses for H_2O and CO_2 established this cordierite's composition to be

$$K_{0.00}Na_{0.05}(Mg_{1.94},Fe_{0.08},Mn_{0.01})$$
$$Al_{3.97}Si_{4.99}O_{18}[0.33\ H_2O,0.08\ CO_2]$$

prior to heating. After heating, through loss of the volatile channel occupants (and perhaps some Na), it became

$K_{0.01}Na_{0.03}(Mg_{1.91},Fe_{0.09},Mn_{0.01})\ Al_{3.98}Si_{5.01}O_{18}$.

Samples (~50 mg) of this tempered cordierite were sealed in platinum tubes and held for 4 weeks at 600°C under H_2O pressures of 0.5, 2, 4, 5 and 6 kbar. Others were similarly treated but in a CO_2 atmosphere (from decomposition of $Ag_2C_2O_4$). Annealing times of 4 weeks were needed to achieve optical homogeneity within the crystal grains of the sample. The samples were subsequently checked by IR spectroscopy between 5000 cm^{-1} and 400 cm^{-1} using the KBr-powder technique. H_2O and CO_2 were thus easily detected. H_2O displays symmetric and asymmetric stretching modes between 3570 cm^{-1} and 3700 cm^{-1} (Farrell and Newnham, 1967; Goldman *et al.*, 1977). Gaseous CO_2 possesses an asymmetric stretching vibration at 2349 cm^{-1}. Hence, absorption at or near 2354 cm^{-1} for beryl (Wood and Nassau, 1967) and for cordierite (Farrell and Newnham, 1967) was attributed by them to CO_2 trapped in the channels. For the optical studies, single grains from each run were mounted on a goniometer head and oriented on the spindle stage. Refractive indices were measured by the double variation (λ, T) method and $2V$ was calculated from extinction data at 400, 666 and 900 nm applying the computer program EXCALIBR. A precise description of the optical methods used in this paper is given elsewhere (Selkregg and Bloss, 1980; Bloss, 1981). The precision of the refractive indices is within 0.0005 and $2V$ within 0.5°. For the same crystal grains, cell dimensions were measured by the back-reflection Weissenberg method. For at least 60 indexed reflections ($CuK\alpha_1$, $CuK\alpha_2$ and $CuK\beta$), 2θ values were submitted to the least square program of Burnham (1962, 1965), as revised by L. Finger, which corrects for film shrinkage and absorption. Water in the samples was quantitatively determined by the equation of Medenbach *et al.* (1980) which relates change in average refractive index (upon heating to complete dehydration) to water content for Mg-cordierite. CO_2 released from the sample at 1300° C was determined using the same equipment and method as described in detail by Johannes and Schreyer (1980). These CO_2 and H_2O analyses lead to standard deviations below 5% of the total gas analyzed. The orientation of CO_2 in natural cordierites was determined by polarized IR spectroscopy from oriented single crystal slabs kindly provided by D. S. Goldman (and described by Goldman *et al.*, 1977). For these single crystal slabs, we compared the relative intensity of the asymmetric stretching absorption of CO_2 at (*ca.*) 2350 cm^{-1} along the *a*, the *b*, and the *c* axis.

Results

The White Well cordierite, degassed by heating between 1200° and 1300°C in a slightly reducing atmosphere, developed oriented cracks but no color change or accompanying hematite reflections in its X-ray photographs. The cracks subsequently vanished for the H_2O-treated crystals, probably because H_2O enhances diffusion processes. By contrast, the CO_2 treatment caused only partial healing of the cracks. IR spectra confirmed H_2O as the only volatile channel occupant in the H_2O-treated cordierites and CO_2 as the only one in the CO_2-treated ones. The H_2O-containing cordierites show a strong absorption peak at 3690 cm^{-1} and weaker ones at 3575 cm^{-1} and 3630 cm^{-1}. The CO_2-containing cordierites exhibit strong peaks at about 2350 cm^{-1}. There is no significant difference in the frequencies of the absorption bands for channel CO_2 and H_2O observed by us from those observed by Farrell and Newnham (1967) or Goldman *et al.* (1977). Absorption bands attributed to AlO_4, SiO_4, and MgO_6 vibrations are consonant with the spectra observed by Langer and Schreyer (1969). Non-equilibrium conditions during hydration or carbonation were readily detected because the resultant crystals possessed higher refractive indices at their edges than at their cores. Moreover, such non-homogeneous crystals exhibited undulatory extinction because of the strong influence of H_2O and CO_2 on the optic angle (Armbruster and Bloss, 1980). By contrast, crystals annealed at 600°C for 4 weeks displayed sharp extinction.

With increased gas in the channels, each refractive index increased significantly (Fig. 2, Table 1). As channel H_2O increased, β increased more rapidly than γ and much more so than α. Hence, $2V_x$ decreases sharply. As channel CO_2 increased, γ increased much more rapidly than β and α. Hence, $(\gamma-\alpha)$ and $2V_x$ increased strongly with channel CO_2 as first noted by Armbruster and Bloss (1980). CO_2 and H_2O each affect the cell dimensions (Fig. 3, Table 2). Channel H_2O decreases a_o but it slightly increases b_o and c_o so that cell volume remains constant (within the range of error). As a result, the distortion index Δ, calculated by the simplified equation of Selkregg and Bloss (1980), namely

$$\Delta = 1.094\ (a_0 - b_0\sqrt{3})$$

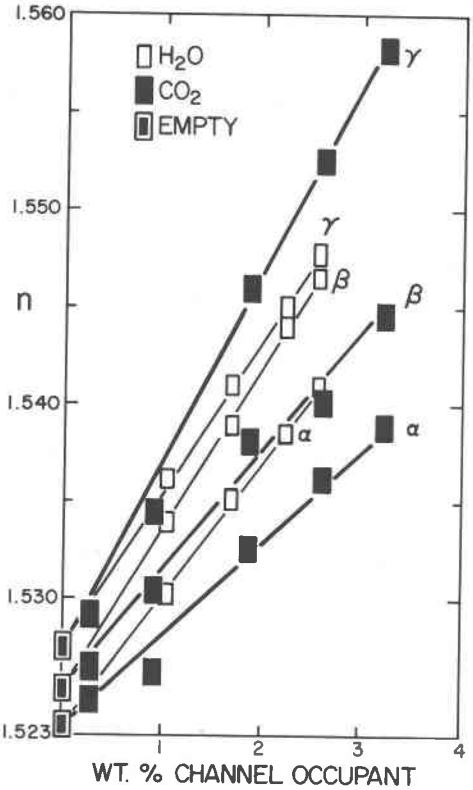

Fig. 2. The increase in refractive index of Mg-cordierite that results if H_2O occupies the channels (light lines, open rectangles) or if CO_2 occupies the channels (bold lines, solid rectangles). The edges of the rectangles correspond to two estimated standard deviations. The data for the channel evacuated cordierite are represented by concentric open and solid rectangles.

decreased as H_2O content increased. With increased channel CO_2, a_0 first decreases but, beyond 2 weight percent CO_2, it increases; b_0 seemed unaffected by CO_2 but c_0 increased strongly. Consequently, Δ decreased (up to 2 weight percent CO_2), then increased slightly.

IR spectra for slabs cut from a crystal of natural cordierite confirmed the conclusions of Farmer (1974) that the linear CO_2 molecule aligns mainly in the (001) plane and, within this plane, chiefly along *a*.

Hartshorne and Stuart (1970, p. 137) state the Lorentz–Lorenz equation for molecular refractivity R_M to be

$$R_M = \frac{n^2 - 1}{n^2 + 2}\frac{M}{\rho} = \frac{4}{3}\pi N P$$

where *n*, *M*, *ρ*, *N* and *P* respectively represent refractive index, molecular weight, density, the Avogadro number, and the electron polarizability for a molecular compound, where *P* is the polarizability averaged over all possible orientations of the electric vector. Although the equation is not strictly applicable to anisotropic crystals, Hartshorne and Stuart note that a principal refractive index (*ε*, *ω*, *α*, *β*, or *γ*) may be substituted for *n*. In such case *P* reasonably approximates the crystal's polarizability along the principal vibration direction associated with this principal index and may thus be symbolized P_ε, P_ω, P_α, P_β or P_γ, as the case may be. For example,

$$P_\varepsilon = \frac{\varepsilon^2 - 1}{\varepsilon^2 + 2} \cdot \frac{M}{\rho} \cdot \frac{3}{4\pi N}$$

Actually, M/ρ represents the molar volume V_M. For a crystal with known unit-cell volume (V_{uc}), if *Z* represents the formula units encompassed by V_{uc}, then its molar volume can be calculated since

$$V_M = \frac{N\,V_{uc}}{Z}$$

Hence the preceding equation can be rewritten as, for example,

$$P_\varepsilon = \frac{3}{4\pi} \cdot \frac{\varepsilon^2 - 1}{\varepsilon^2 + 2} \cdot \frac{V_{uc}}{Z}$$

For mineralogists this is convenient since V_{uc} and *Z* are more likely to be accurately known than density or molecular weight. The units for *P* will be those used for V_{uc} (usually $Å^3$).

For the cordierites here studied, polarizabilities P_α, P_β, and P_γ were calculated using their principal

Table 1. Optical data of H_2O and CO_2 treated White Well cordierite at 600°C.

Pressure (kbar)	Gas (wt %)	α	β	γ	$\bar{n}$	(γ - α)	$2V_x$*
Channel-evacuated							
--	--	1.5235	1.5254	1.5275	1.52546	0.0040	87.0
H_2O re-introduced into channels							
0.5	1.05	1.5303	1.5340	1.5362	1.53350	0.0059	64.6
2.0	1.68	1.5351	1.5389	1.5410	1.53833	0.0059	56.6
4.0	2.24	1.5386	1.5440	1.5450	1.54253	0.0064	50.0
6.0	2.56	1.5409	1.5465	1.5477	1.54503	0.0068	44.1
CO_2 re-introduced into channels							
0.5	0.27	1.5238	1.5260	1.5287	1.52616	0.0049	86.8
2.0	0.91	1.5263	1.5305	1.5345	1.53043	0.0082	93.8
4.0	1.88	1.5326	1.5381	1.5459	1.53887	0.0133	105.0
5.0	2.61	1.5362	1.5410	1.5525	1.54323	0.0163	111.1
6.0	3.13	1.5388	1.5446	1.5582	1.54720	0.0187	112.4

* Average of measurements at 400, 666, and 900 nm

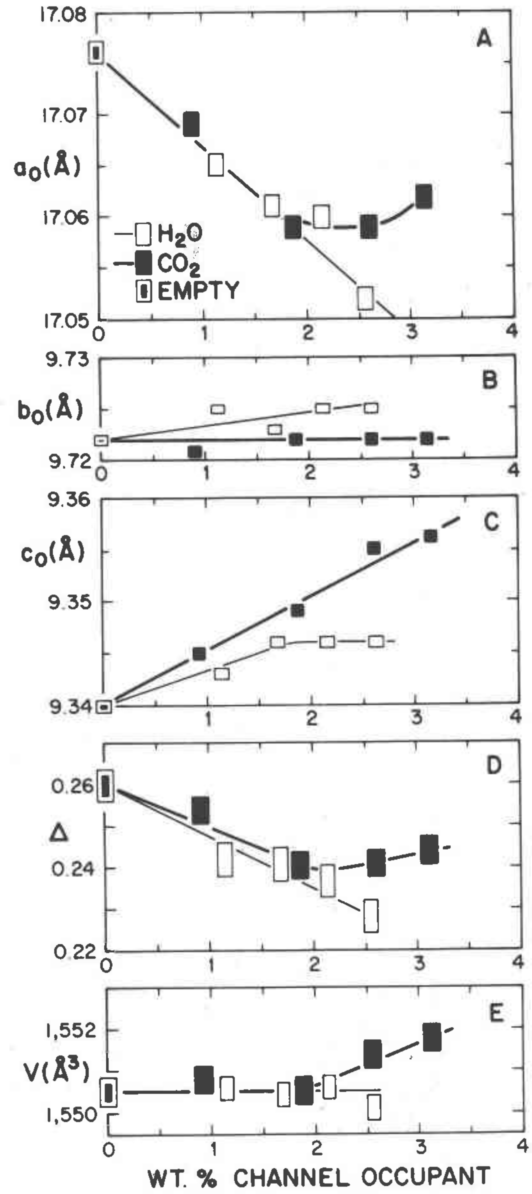

Fig. 3. Variation in unit cell edges (A, B and C), distortion index Δ (D), and unit cell volume (E) as amount of channel occupant increases. The rectangles have the same significance as in Figure 2.

indices for sodium light (α_D, β_D, and γ_D), V_{uc}, and Z (Table 3). These polarizabilities increase systematically with increased weight per cent of channel H_2O or CO_2 (Fig. 4). The trends indicate that as channel H_2O increases, cordierite's polarizabilities (and associated refractive indices) increase at the greatest rate for light vibrating parallel to Y, at a lesser rate for Z, and at the least rate for X. With increase in channel CO_2, the polarizabilities (and associated indices) increase most rapidly for Z (= a axis), least for X (= c axis) and, for Y (= b axis), at a slightly greater rate than that for X. The marked increase in polarizability along Z, as CO_2 increases, underscores (1) the ready polarizability of the linear CO_2 molecule along its length and, as IR spectra indicate, (2) the tendency of this molecule to align chiefly parallel (or subparallel) to the a axis in cordierite. This causes ($\gamma-\alpha$) and $2V_x$ to increase with channel CO_2 content.

The linearity of the trends in Figure 4 reinforce confidence in the measurement of the refractive indices and in the determinations of H_2O and CO_2. However, specimens with a relatively low content of H_2O and CO_2 seem at variance with these trends. Such variance may result (1) from experimental errors in determining CO_2 or H_2O, or (2) from a possible tendency of channel CO_2 or H_2O molecules to orient somewhat differently at low concentrations as compared to high.

Discussion

From IR spectra of 8 natural cordierites, Goldman *et al.* (1977) confirmed two major types of orientation for the H–H vector for channel water—H–H parallel c (type I) or H–H parallel b (type II)—and noted that absence of channel cations, especially Na, favors type I. Tsang and Ghose (1972) investigated a Mg-rich cordierite from Madagascar by NMR technique and found only type I water. The relatively high distortion index (Δ = 0.24) calculated from the cell dimensions, suggests this specimen to be Na-poor (Selkregg and Bloss, 1980).

Table 2. Cell dimensions, volume and distortion index of H_2O and CO_2 treated White Well cordierite at 600°C*

Pressure (kbar)	Gas (wt %)	a_o [Å]	b_o [Å]	c_o [Å]	V [Å³]	Δ
			Channel-evacuated			
—	—	17.076$^{(2)}$	9.722$^{(1)}$	9.340$^{(1)}$	1550.5$^{(3)}$	0.260$^{(3)}$
			H_2O re-introduced into channels			
0.5	1.05	17.065	9.725	9.343	1550.6	0.242
2.0	1.68	17.061	9.723	9.346	1550.4	0.241
4.0	2.24	17.060	9.725	9.346	1550.6	0.237
6.0	2.56	17.052	9.725	9.346	1550.1	0.228
			CO_2 re-introduced into channels			
0.5	0.27	—	—	—	—	—
2.0	0.91	17.069	9.721	9.345	1550.8	0.254
4.0	1.88	17.059	9.722	9.349	1550.5	0.241
5.0	2.61	17.059	9.722	9 355	1551.1	0.241
6.0	3.13	17.062	9.722	9.356	1551.8	0.244

* Numbers in parentheses in the table represent the estimated standard deviation in terms of the least decimal place cited for the value to the left and for all other values in the column below. The precisions achieved in determining the gas contents are discussed in the text.

Table 3. Polarizabilities for the H_2O and CO_2 treated White Well cordierite

Gas (wt %)	P_α (Å³)	P_β (Å³)	P_γ (Å³)	$P_{\bar{n}}$ (Å³)
Channel-evacuated				
--	28.291	28.377	28.472	28.380
H_2O re-introduced into channels				
1.05	28.601	28.767	28.866	28.745
1.68	28.813	28.983	29.077	28.958
2.24	28.973	29.215	29.259	29.149
2.56	29.067	29.317	29.370	29.251
CO_2 re-introduced into channels				
0.27	28.310	28.410	28.532	28.420
0.91	28.424	29.613	29.793	28.610
1.88	28.702	28.949	29.298	28.984
2.61	28.875	29.090	29.602	29.190
3.13	29.005	29.264	29.868	29.380

The increase in refractive indices as channel H_2O is reintroduced into channel-evacuated White Well cordierite (Table 3) is consonant with type I water. For this orientation, vectors drawn from the hydrogens to the nearest oxygens of the $Al_2Si_4O_{18}$ rings would represent directions of maximum (but weak) polarization of these oxygens by the hydrogens. Such directions, being more nearly parallel than perpendicular to (001), would hence favor, as Table 3 shows, a greater rate of increase of the indices β and γ than of α with increased channel water (since $X = c$). The long distance (3.4Å) between the water oxygen and the nearest oxygen of the $Al_2Si_4O_{18}$ ring precludes the existence of hydrogen bonding because, when hydrogen bonds exist, the associated O–O distances usually equal 2.7–2.8Å (Vinogradov and Linell, 1971). Moreover, Langer and Schreyer (1976) point out that the slight energy decrease of about 80 cm^{-1} (0.2 kcal) for the IR-stretching modes of H_2O in cordierite compares to those for H_2O vapor, this again indicating unlikelihood of strong hydrogen bonds, these latter usually being in the range of 5 kcal.

The linear CO_2 molecule (4.96Å) has been observed with its elongation mostly normal to the *c* axis (Farrell and Newnham, 1967) and only to a smaller degree parallel to *c* (Farmer, 1974). Our IR results confirm this. Such observations of the orientation of CO_2 (and H_2O) in natural specimens may be complicated because specific CO_2 and H_2O orientations may result from interaction with other channel occupants (or each other). On the other hand, the small shifts of the CO_2 bands in IR spectra for cordierite as compared to those of CO_2 in the gaseous state suggest only minor interaction with the silicate framework. The marked increase in the refractive index γ, as channel CO_2 is reintroduced into a channel-evacuated White Well crystal (Table 3), suggests that CO_2 is dominantly aligned parallel to *a* (= *Z*). The refractive index α displays the least

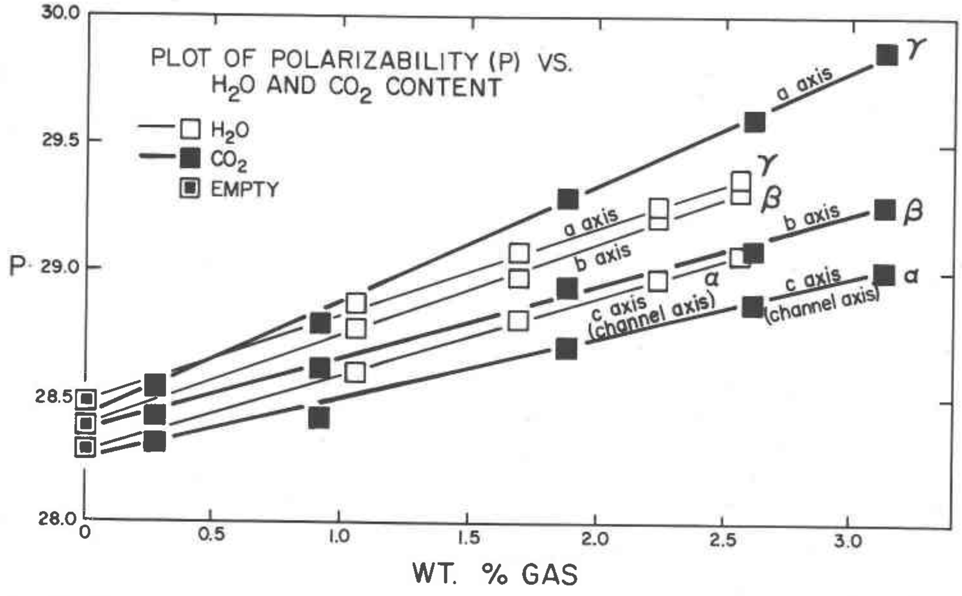

Fig. 4. Variation of the Lorentz-Lorenz polarizability *P* (in Å³) for White Well cordierite crystals as their channels are increasingly occupied by H_2O (hollow squares) and by CO_2 (solid squares). Estimated standard deviations are not implied by the size of the squares.

rate of increase with channel CO_2. This suggests that CO_2 is dominantly aligned perpendicular to *c* (since $X = c$), even when not parallel to *a*, and thus agrees with the IR results.

Elongation of the CO_2 molecule parallel to *a* (type *a* orientation) avoids strong interaction with the oxygens that form the channel walls and with any other CO_2 molecules in the cavities above or below (Fig. 5A). The most probable position for CO_2, if oriented parallel to *c* (type *c* orientation), is with its carbon centered within the $Al_2Si_4O_{18}$ ring (Fig. 5B) so that its oxygen atoms extend into the cages. In such case, however, only every second cavity could be occupied by CO_2 because $c_o/2$ equals 4.7Å whereas the length of CO_2 is 4.96Å. Type *c* orientation might be favored by a low degree of channel filling, perhaps coupled with presence of cations (Na^+, *etc.*) in adjacent available sites.

With increased re-introduction of channel CO_2, a_o initially decreased but then increased, b_o remained constant, and c_o increased significantly (Table 2, Fig. 3). With increased channel H_2O, a_o decreased, b_o perhaps increased slightly, and c_o initially increased but then levelled off. Channel H_2O and channel CO_2 both decreased the distortion index Δ (Table 2).

Under the same *P–T* conditions, fewer CO_2 molecules than H_2O molecules enter cordierite's channels. At 600°C and 6 kbar, approximately twice as many H_2O molecules as CO_2 molecules enter (so that the number of oxygens entering is about the same in each case). Presumably, the elongate CO_2 molecule enters the channel like a needle entering a tube of slightly larger diameter. After reaching a cavity, the CO_2 molecule must rotate 90° to become parallel to *a*, its favored orientation. With heating to expel CO_2 from the channels, any CO_2 molecule aligned along *a* must rotate 90° in order to diffuse outward along the channels or else decompose to smaller breakdown products.

Puzzingly, at 600°C and 5 kbar, we observed 2.61 wt.% CO_2 to enter the White Well cordierite whereas Johannes and Schreyer (1980) observed that, under these same *P–T* conditions only 1 wt.% CO_2 entered finely powdered synthetic Mg-cordierite. In each case the same equipment and methods were used to determine CO_2. Possible synthetic cordierites possess a greater frequency of channel offsets or dislocations (by twin, domain, or grain boundaries). Also, Johannes and Schreyer (1980), using two different types of synthetic Mg-cordierites, noted a pronounced effect of the starting material on the amount of CO_2 (but not H_2O) that entered. For natural cordierites, on the other hand, the effect of channel Na or of Fe content upon entry of CO_2 is not as yet known. A catalytic interaction between Na and CO_2 might favor incorporation of CO_2 into the channels. These conjectures aside, the internal consistency of our optical data, which yield Lorentz–Lorenz polarizabilities that plot quite linearly relative to wt.% CO_2 (Fig. 4), corroborate a value of 2.61 wt.% CO_2 for the grain held at 600°C, 5 kbar in a CO_2 atmosphere.

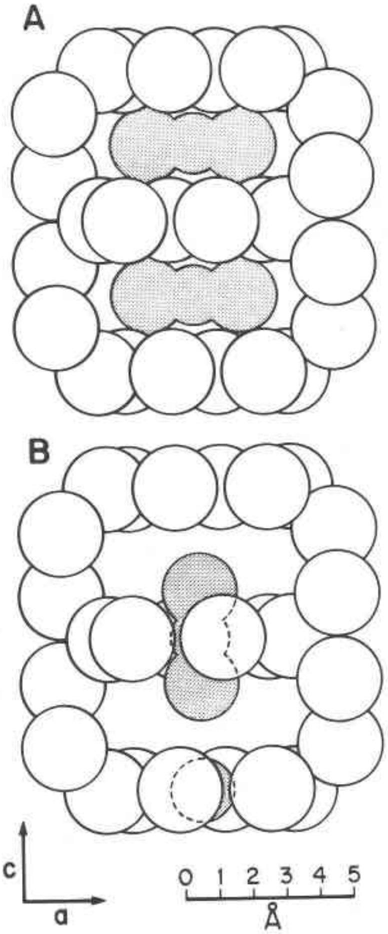

Fig. 5. A portion of the cordierite structure, viewed down the *b*-axis, showing only those oxygen atoms that form a single channel in the cordierite framework. Three "bottlenecks" are thus viewed edgewise, and midway between the centers of each two bottlenecks are the large open cages. (A) A CO_2 molecule (shaded dark) is shown in its preferred position (parallel to the *a*-axis) in the cage. (B) A CO_2 molecule oriented parallel to the *c*-axis, an orientation considerably less frequent that than in (A). Centered in the lowest ring is an almost completely obscured sodium atom (shaded where seen).

Knowledge of the effect of CO_2 and H_2O on the optical properties of cordierites may enable us (Armbruster and Bloss, in preparation) to estimate the absolute and/or relative amounts of H_2O and CO_2 in natural cordierites. Ultimately, it is hoped, such data may provide estimates of the composition of the fluid phase with which a cordierite was last in equilibrium.

Acknowledgments

This research was supported in part by NSF grant EAR 8018492 (to FDB) and in part by a grant from the Deutsche Forschungsgemeinschaft (to ThA). We thank Drs. George Rossman and Donald Goldman for loan of the single crystal slabs of cordierite and Dr. Lucian Zelazny for use of the IR equipment in his laboratory. We are grateful to Professor Werner Schreyer and to the Institut für Mineralogie, Ruhr Universität Bochum for help with the CO_2 analyses.

References

Armbruster, Th. and Bloss, F. D., (1980) Channel CO_2 in cordierites. Nature, 286, 140–141.

Ambruster, Th. and Bloss, F. D., (1981) Mg-cordierite: Si/Al ordering, optical properties, and distortion. Contributions to Mineralogy and Petrology, 77, 332–336.

Beltrame, R. J., Norman, D. I., Alexander, E. C., and Sawkins, F. J. (1976) Volatiles released by step-heating a cordierite to 1200°C Transactions American Geophysical Union, 57, 352.

Bloss, F. D. (1981) The spindle stage. Cambridge University Press, Cambridge and New York.

Burnham, C. W. (1962) Lattice constant refinement. Carnegie Institution of Washington Year Book, 61, 132–135.

Burnham, C. W. (1965) Refinement of lattice parameters using systematic correction terms. Carnegie Institution of Washington Year Book, 64, 200–202.

Cohen, J. P., Ross, F. K, and Gibbs, G. V., (1977) An X-ray and neutron diffraction study of hydrous low-cordierite. American Mineralogist, 62, 67–78.

Damon, P. E. and Kulp, J. L. (1958) Excess helium and argon in beryl and other minerals. American Mineralogist, 43, 433–459.

Farmer, V. C. (1974) The infrared spectra of minerals, Mineralogical Society, London.

Farrell, F. and Newnham, R. E., (1967) Electronic and vibrational absorption spectra in cordierite. American Mineralogist, 52, 380–388.

Gibbs, G. V. (1966) The polymorphism of cordierite I: the crystal structure of low cordierite. American Mineralogist, 51, 1068–1087.

Goldman, D. S., Rossman, G. R., and Dollase, W. A., (1977) Channel constituents in cordierite. American Mineralogist, 62, 1144–1157.

Hartshorne, N. H., and Stuart, A., (1970) Crystals and Polarising Microscope, Edward Arnold Ltd., London.

Hochella, M. F., Brown, G. E., Ross, F. K., and Gibbs, G. V. (1979) High temperature crystal chemistry of hydrous Mg- and Fe-cordierites. American Mineralogist, 64, 337–351.

Hörmann, P. L., Raith, M., Raase, P., Ackermand, D., and Seifert, F., (1980) The granulite complex of Finnish Lapland: Petrology and metamorphic conditions in the Ivalojoki-Inarijärvi area, Finland Geological Survey Bulletin, 308, 1–95.

Johannes, W. and Schreyer, W., (1980) Experimental introduction of CO_2 and H_2O into Mg-cordierite. American Journal of Science, 281, 299–317.

Langer, K., and Schreyer, W., (1969) Infrared and powder X-ray diffraction studies on the polymorphism of cordierite, $Mg_2Al_4Si_5O_{18}$. American Mineralogist, 54, 1442–1459.

Langer, K., and Schreyer, W., (1976) Apparent effects of molecular water on the lattice geometry of cordierite: a discussion. American Mineralogist, 61, 1036–1040.

Lee, J. D., and Pentecost, J. L., (1976) Properties of flux-grown cordierite single crystals. Journal of the American Ceramic Society, 59, 182.

Meagher, E. P. (1967) The Crystal Structure and Polymorphism of Cordierite. Ph.D. Dissertation, The Pennsylvania State University, University Park, Pennsylvania.

Meagher, E. P. and Gibbs, G. V., (1977) The polymorphism of cordierite. II. The crystal structure of indialite. Canadian Mineralogist, 15, 43–49.

Medenbach, O., Maresch, W., Mirwald, P., and Schreyer, W. (1980) Variation of refractive index of synthetic Mg-cordierite with H_2O. American Mineralogist, 65, 367–373.

Miyashiro, A. (1957) Cordierite-indialite relations. American Journal of Science, 255, 43–62.

Miyashiro, A., and Iiyama, T., (1954) A preliminary note on a new mineral, indialite, polymorphic with cordierite. Proceedings of Japan Academy, 30, 746–751.

Povondra, P., and Langer, K., (1971) Synthesis and properties of sodium-beryllium-bearing cordierite, $Na_xMg_2(Al_{4-x}Be_xSi_5O_{18})$ Neues Jahrbuch für Mineralogie, Abhandlungen, 116, 1–19.

Pryce, M. W. (1973) Low-iron cordierite in phlogopite schist from White Well, Western Australia. Mineralogical Magazine, 39, 241–243.

Putnis, A. (1980) Order-modulated structures and the thermodynamics of cordierite reactions. Nature, 287, 128–131.

Schreyer, W., and Schairer, J. F., (1961) Composition and structural state of anhydrous Mg-cordierites: a re-investigation of the central part of the system $MgO–Al_2O_3–SiO_2$. Journal of Petrology, 2, 324–406.

Schreyer, W., and Yoder, H. S., (1964) The system Mg-cordierite-H_2O and related rocks, Neues Jahrbuch für Mineralogie, Abhandlungen, 101, 271–342.

Schreyer, W., Gordillo, C. E., Werding, G., (1979) A new sodian beryllian cordierite from Soto, Argentina, and the relationship between distortion index, Be-content, and state of hydration. Contributions to Mineralogy and Petrology, 70, 421–428.

Selkregg, K. R., and Bloss, F. D., (1980) Cordierites: compositional controls of Δ, cell parameters, and optical properties. American Mineralogist, 65, 522–533.

Suknev, V. S., Kizul, V. I., Lazebnik, Yu. D., and Brovkin, A. (1971) Akademii NAUK SSSR, Doklady, 20, 950–952 (in Russian).

Tsang, T., and Ghose, S., (1972) Nuclear magnetic resonance of ^1H and ^{27}Al and Al-Si order in low cordierite $Mg_2Al_4Si_5O_{18} \cdot n H_2O$. Journal of Chemical Physics, 56, 3329–3332.

Vinogradov, S. N. and Linell, R. H., (1971) Hydrogen Bonding, Van Nostrand Reinhold, New York.

Wallace, J. H., and Wenk, H. R., (1980) Structure variation in low cordierites. American Mineralogist, 65, 96–111.

Wood, D. L., and Nassau, K., (1967) Infrared spectra of foreign molecules in beryl. Journal of Chemical Physics, 47, 2220–2228.

Manuscript received, August 17, 1981;
accepted for publication, November 30, 1981.